Developing a main bearing load estimation model to predict reliability of next-generation offshore wind turbines

Daniyal Jamal

Office of Science, Science Undergraduate Laboratory Internship Program
Stony Brook University, Stony Brook, NY

National Renewable Energy Laboratory
Golden, Colorado

December 11, 2020

Prepared in partial fulfillment of the requirement of the Department of Energy, Office of Sciences Science Undergraduate Laboratory Internship Program under the direction of Dr. Caitlyn Clark at the National Renewable Energy Laboratory.

Participant: Daniyal Jamal

Research Advisor: Dr. Caitlyn Clark

Abstract

Main bearings in offshore wind turbines are predicted to be an increasing source of failure and cost as these turbines accelerate in deployment, grow in capacity and size, and gradually adopt direct-drive systems while being installed increasingly farther from shore. Larger components and harsh offshore wind conditions increase loads on, and dynamic responses of, particular components, while also being more difficult and costly to repair given their increasing component size and distance from shore. Collectively, these industry trends could result in greater O&M costs and downtime if changes in loads and failure are not addressed. To improve component reliability and optimize O&M strategies, predictive models are required for main bearing failure. In this study, an accurate, low-fidelity, computationally-efficient main bearing load estimation model is developed and validated. Model parameters for the modified 5-MW, IEA 10-MW, and IEA 15-MW reference wind turbines are presented in this study. This model employs wind turbine simulation data and reference wind turbine parameters to estimate wind turbine main bearing reliability from the calculated loads. This open-source tool will enable researchers to consider main bearing reliability in optimization and design studies, O&M simulations, and other analyses that require tens of thousands of evaluations to reach a final solution.

I. INTRODUCTION

The offshore wind energy sector is a relatively new and rapidly growing market with a global capacity of 29.1 GW.[1] As of 2019, over 6.4 GW of offshore projects are currently in the planning pipeline in the United States, with projected growth expected to increase as west coast installations begin.[2] The rapid growth of the offshore wind energy market has been partially enabled by the increasing power generation capacity and size of wind turbines. In 2019, the average turbine capacity for offshore wind energy was 6 MW with a rotor diameter of 100 meters, however, projections show these numbers increasing to 11 MW and 200 meters, respectively, by 2025.[2] The growth and potential of offshore wind is evident in current market reports.

With these new opportunities, offshore locations pose new engineering challenges as well. As wind turbines move offshore, they can be designed to be significantly larger with greater capacities due to different space availability and visual impact constraints as compared to onshore installations. In addition, wind speeds are higher and more consistent offshore, leading to annual yields of up to 50% more electricity than onshore wind turbines of equal capacity and type.[3] The increase in wind resource and component size promises greater energy production, but also subjects turbine components to greater loads, which, without consideration in design, could lead to greater failure. As O&M costs are reported to be as high as 35% of total lifetime costs of offshore wind projects, reducing failure rates is critical to project bankability.[4] In addition to increased component failure, increased O&M costs offshore are exacerbated by reduced accessibility in harsh ocean conditions as well as the availability of specialized vessels, technicians, and parts required for frequent maintenance and repair.[5] Offshore wind turbines experience significantly higher failure rates than onshore wind projects because of higher wind speeds and larger capacity of turbines offshore.[6] Wind turbine component reliability remains a major concern as offshore wind deployment accelerates.

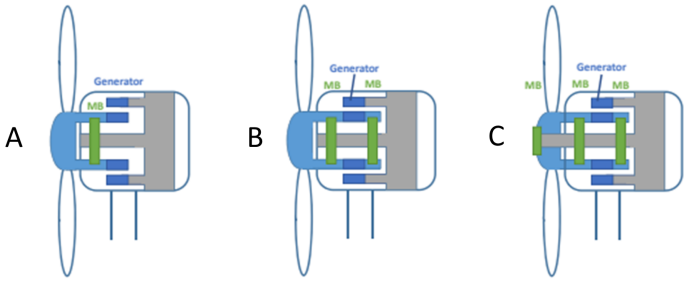

Figure 1: Depictions of existing drivetrain layouts for direct-drive turbines with an example of single (A), double (B), and triple (C) main bearing design[7]

One component that is predicted to be a significant and increasing source of failure in future offshore wind development is the main bearing. Main bearing configuration can differ and examples of drivetrain layouts for direct-drive systems can be seen in Figure 1. The main bearings in wind turbines employ rolling elements to constrain relative motion between the turret and main shaft, allowing the turbine rotor to rotate with minimal friction. This component interacts with both the rotor and drivetrain, and thus is affected by the aerodynamic and torque loads from the wind field as well as the non-torque load from the drivetrain.[7] Main bearings are a high-risk component, with studies that report failure rates at nearly 30% over a 20-year lifetime.[8] Main bearings have shown increasing evidence of failure, with many turbine bearings failing to survive beyond 6 years.[9] Wind turbines that employ spherical roller bearings (SRB) are especially susceptible to micropitting, single-piece cage failure, roller edge loading, and debris damage, as seen in Figure 2.[10]

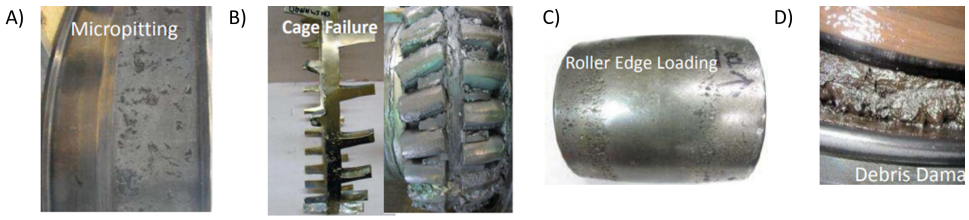

Figure 2: SRB failure modes[9]

These failure modes inevitably compromise system operation, leading to expensive repairs and downtime. For reference, the presence of micropitting on the main bearing rollers can result in repair costs of 150k to 300k USD2013.[11] The leading failure modes of the main shaft involve the fatigue or wear of raceways and rollers, primarily due to microgeometry, local overload, and lack of lubrication.[12] Fatigue is one of the most prominent failure modes for the main bearings, causing plastic deformation and fatigue cracking, which often triggers other failure mechanisms.[7,12] Therefore, improving and predicting reliability is essential in planning for O&M, reducing lifetime costs, and making offshore wind energy more competitive in the energy market. Additionally, accurate

modeling of main bearing loads and estimation of failure will enable original equipment manufacturers and operators to reduce failure as well as optimize O&M strategies.

Previous work in predicting drivetrain loads and reliability vary in complexity, fidelity, and computational expense. Wind turbines are subjected to fluctuating loads and vibrations which propagate throughout the structure and drivetrain.[13] Predictive modeling and simulations are critical in considering the increased loads and stresses caused by larger turbine components and harsh wind conditions present offshore.[14,15] As highlighted by Li et al., the dynamic loads are currently analyzed using the following approaches: (1) pure torsional rigid models, (2) multi-degree-of-freedom rigid models, (3) flexible multibody models.[16] Often, torsional rigid multibody models, which do not account for lateral loads in the drivetrain, are not sufficient to produce realistic results. On the other hand, flexural dynamic models which consider the elasticity of each gear, carrier, and housing in the drivetrain, are computationally expensive.[17] Previous studies in main bearing modeling often employed high-fidelity methods which cannot be applied in iterative models and optimization studies. These approaches include Hertzian elastic contact theory, finite element models, and multi-body simulations.[7] Additionally, multiple past studies have overlooked the main bearing or included it under larger systems such as the "drivetrain" or "main shaft" in modeling and failure analysis.[12,16,18] Further research is needed to develop a low-fidelity, computationally-efficient main bearing model that can easily be integrated into systems design and optimization analyses.

This study develops an accurate, open-source, computationally-inexpensive main bearing analytical model to predict fatigue loads and reliability. This model leverages aeroelastic simulation data as well as reference wind turbine (RWT) parameters to estimate loads and reliability in wind turbine main bearings. As seen in Figure 3, the three RWTs, the modified 5-MW, IEA 10-MW, and IEA 15-MW, play a key role in building the aeroelastic simulations, providing drivetrain parameters for the analytical model, and also providing main bearing parameters for the reliability model. These RWT parameters are collated and defined in the Section II.. Using the bearing loads calculated by the analytical model and main bearing parameters, bearing reliability is quantified using the L_{10} life metric. Section C. describes the validation method used to verify the analytical model. The product of this study is the accumulation of drivetrain and main bearing parameters of previous RWTs and a versatile tool for main bearing modeling. Developed as part of the Reliability-Based Layout Optimization software,[19] this work allows for the consideration of main bearing loads and reliability in layout and controls optimization of wind plants for three RWTs. This work also enables researchers to integrate main bearing reliability into O&M simulations, design and optimization, and other iterative analyses, which may ultimately improve main bearing reliability, reduce wind turbine life time costs, and accelerate offshore wind deployment to reduce carbon emissions.

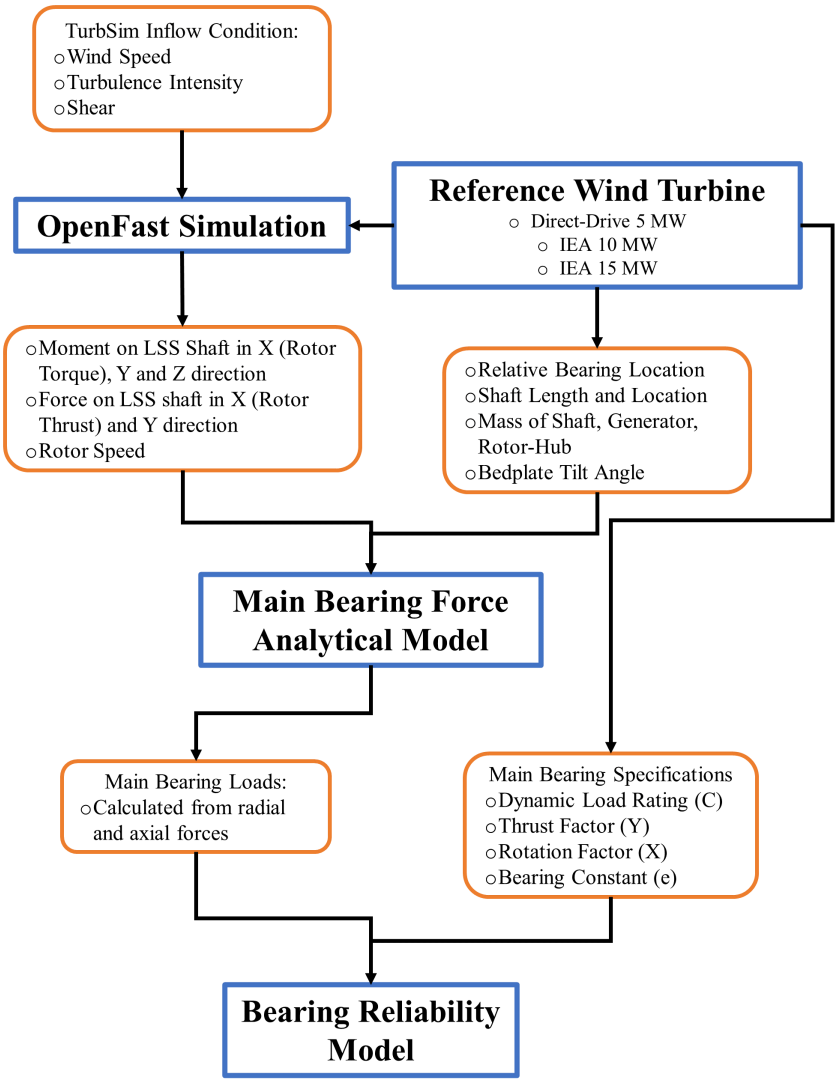

Figure 3: The flow of data through models used in this study

II. Methods

In this section, the IEA 15-MW, IEA 10-MW, and the modified 5-MW RWT used in this study are first presented. Key drivetrain parameters are gathered and established for each RWT. Additionally, main bearing specifications are obtained from previous research or established through design for each RWT. Next, the model formulation and force diagram is presented along with specific simulation parameters used in the model. This is followed by the model validation method and lastly, the bearing reliability calculations. The flow of data and parameters through each model used in this study can be seen in Figure 3.

A. Reference Wind Turbines

RWTs serve an important role in enabling access for researchers to current wind turbine analysis methods and design specifications. RWTs are defined with publicly-

available design parameters meant to be used as baselines for future studies to explore new wind turbine technologies and design.

1. IEA 15-MW Offshore RWT

The 15-MW RWT[20] is rated for Class IB, a high-wind, low-turbulence offshore wind rating. This turbine is a direct-drive machine with a fixed-bottom monopile support structure. The 15-MW RWT has a rotor diameter of 240 meters and a hub height of 150 meters. The relevant drivetrain parameters for the 15-MW RWT are provided in Table 1. The IEA 15-MW RWT 3D CAD model uses a product by Timken to model the main bearings. For this study, the bearing parameters are scaled and derived from this main bearing selection, and are shown in Table 1.

Table 1: IEA 15-MW RWT Parameters

Parameter	Variable	Value	Units
Mass of Generator	m_{gr}	371592	kg
Mass of Shaft	m_s	15734	kg
Mass of Rotor and Hub	m_{rh}	385000	kg
Bedplate Tilt Angle	ρ	6	degrees
Distance from MB1 and MB2	L_g	1.2	meters
Distance from Generator to MB1	L_{gr}	0.9	meters
Distance from Shaft to MB1	L_s	0.25	meters
Distance from Hub to MB1	L_r	3.638	meters
Hub Overhang	L_h	11.35	meters

Table 2: IEA 15-MW Offshore RWT Main Bearing Specification

Scaled Timkin EE755285 - 755367CD[21]	Variable	Value	Units
Basic Dynamic Load Rating	C	25926	kN
Basic Static Load Rating	C_0	108170	kN
Fatigue Load Limit	P_u	4760	kN
Radial Load Factor	X	0.39	-
Axial Load Factor	Y	0.45	-

2. IEA 10-MW Offshore RWT

The 10-MW offshore RWT was developed for the IEA Wind Task 37.[22] This design is derived from the DTU 10-MW RWT with identical nominal power capacity and wind class rating.[23] The primary distinction of the 10-MW offshore wind turbine is its direct-drive system. Table 3 shows certain parameters obtained from the technical report that are used in the analytical model.

The main bearings for the 10-MW offshore RWT are designed and specified by Smith.[24] However, this method employed by Smith does not consider RWT main shaft and turret diameter in the selection of main bearings. The main bearing parameters for the direct-drive 10-MW RWT are shown in Tables 5 and 4.

Table 3: IEA 10-MW Offshore RWT Drivetrain Parameters

Parameter	Variable	Value	Units
Mass of Generator	m_{gr}	357300	kg
Mass of Shaft	m_s	78894	kg
Mass of Rotor and Hub	m_{rh}	224807	kg
Bedplate Tilt Angle	ρ	5	degrees
Distance from MB1 and MB2	L_g	4.62	meters
Distance from Generator to MB1	L_{gr}	-0.78	meters
Distance from Shaft to MB1	L_s	1.25	meters
Distance from Hub to MB1	L_r	3.618	meters
Hub Overhang	L_h	10.039	meters

Table 4: IEA 10-MW Offshore RWT Front Main Bearing Specification

SKF BT2B 332497/HA4[25]	Variable	Value	Units
Basic Dynamic Load Rating	C	34700	kN
Basic Static Load Rating	C_0	108000	kN
Fatigue Load Limit	P_u	5000	kN
Radial Load Factor	X	0.56	-
Axial Load Factor	Y	0.72	-

Table 5: IEA 10-MW Offshore RWT Back Main Bearing Specification

SKF 248/1800 CAK30FA/W20[26]	Variable	Value	Units
Basic Dynamic Load Rating	C	20274	kN
Basic Static Load Rating	C_0	63000	kN
Fatigue Load Limit	P_u	3050	kN
Radial Load Factor	X	4.5	-

3. Modified Direct-Drive 5-MW RWT

The mechanical system of an offshore, direct-drive 5-MW wind turbine was designed and analyzed by Sethuraman et al.[27] This design is derived from the original 5-MW, offshore RWT.[28] Sethuraman et al. presents mechanical properties as well as detailed dimensions of the drivetrain. Table 6 reports necessary parameters referenced from this publication.

To specify the main bearings for the 5-MW RWT, the method used by Smith was employed, which leverages aero-elastic simulation data under specific design load conditions to obtain main bearing loads, and then sizes the main bearings based on two requirements: (1) safety factor for static load to static equivalent load must be at least 2, and (2) minimum bearing life must be 20 years given the ultimate loads presented in the study.[24] This same approach is used to size the main bearings for the 5-MW RWT using aero-elastic simulation data under normal load conditions from previous research.[29] This design approach yields the main bearings specified on Tables 8 and 7.

Table 6: Modified 5-MW RWT Drivetrain Parameters

Parameter	Variable	Value	Units
Mass of Generator	m_{gr}	131000	kg
Mass of Shaft	m_s	28500	kg
Mass of Rotor and Hub	m_{rh}	224807	kg
Bedplate Tilt Angle	ρ	5	degrees
Distance from MB1 and MB2	L_g	2	meters
Distance from Generator to MB1	L_{gr}	-0.85	meters
Distance from Shaft to MB1	L_s	-0.85	meters
Distance from Hub to MB1	L_r	0.65	meters
Hub Overhang	L_h	4	meters

Table 7: Modified 5-MW RWT Front Main Bearing Specification

SKF BT2B 332493/HA4[30]	Variable	Value	Units
Basic Dynamic Load Rating	C	8090	kN
Basic Static Load Rating	C_0	16000	kN
Fatigue Load Limit	P_u	1060	kN
Radial Load Factor	X	0.77	-
Axial Load Factor	Y	0.67	-

Table 8: Modified 5-MW RWT Back Main Bearing Specification

SKF 230/750 CA/W33[31]	Variable	Value	Units
Basic Dynamic Load Rating	C	10061	kN
Basic Static Load Rating	C_0	18600	kN
Fatigue Load Limit	P_u	1100	kN
Radial Load Factor	X	3.2	-

B. Model Formulation

The following analytical formulation was adapted from Smith and the DNV guidelines to determine the reaction forces at the main bearings.[24,32] In the formulation of this model, the following assumptions were made:

1. The loads from the aeroelastic simulation are transmitted to the bearing via the main shaft. Bearing forces consists of one axial force and two radial forces in a double main bearing configuration

2. The thrust loads are transmitted by the main shaft to the upwind main bearing only

3. The self-aligning feature of spherical main bearing, which allow misalignment of 1-2.5 degrees, was determined to be sufficient to compensate for deformation, in accordance with DNV guidelines

4. The load sharing, clearances, as well as torsional and vibration dynamics are not considered.

The dynamic loads and moments on the low speed shaft are simulated using OpenFAST, although other aero-elastic simulation tools can be used.[33] The flow field for OpenFAST was generated with TurbSim, with an inflow wind speed of 12 m/s, a turbulence intensity (TI) of 10%, and a shear exponent value of 0.1. Dynamic loads on the low speed shaft, such as the rotor torque, rotor thrust, and bending moments/forces in the y- and z- direction, are then translated to the main bearing components using the analytical component model.

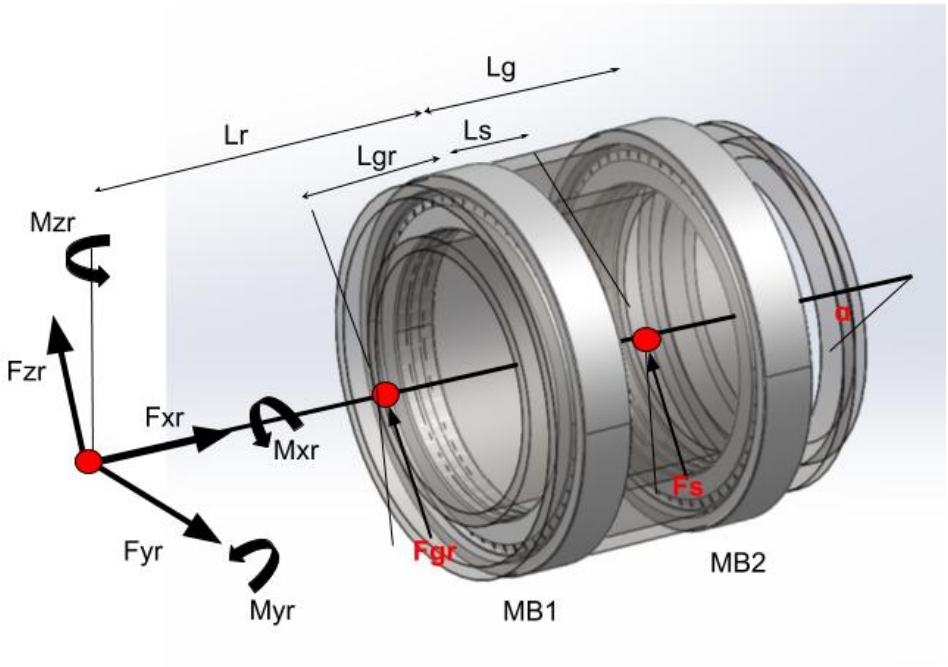

Figure 4: Force and moment diagram of wind turbine shaft with double main bearings

With the OpenFAST data, the reaction forces on the main bearings can be calculated using simple beam theory and static equations. The force and moment diagram is shown in Figure 4. Obtaining the summation of moments about the y- and z-axis relative to the upwind bearing (MB1) results in Equation 1 and Equation 2. Thus, the root-sum-square of these two input moments is equated to the reaction moment present in the downwind bearing (MB2). The radial force on MB2 (Fr2) can then be derived from this moment. The upwind main bearing is subjected to the same radial force (Fr2) in addition to the resultant of the orthogonal forces in the y- and z-direction at the hub. The axial forces, which is only present at MB1, can be found with the summation of forces in the x-direction. The labeled lengths shown in Figure 4 indicate the distance between the wind turbine bearings and the center of mass of components such as the shaft, generator, and hub.

$$M_1 = M_{yr} - F_{zr}cos(\rho)L_r - F_{gr}cos(\rho)L_{gr} + F_s cos(\rho)L_s \tag{1}$$

$$M_2 = F_{yr}L_r + M_{zr} \tag{2}$$

$$F_{r2} = \frac{1}{L_g}\sqrt{M_1^2 + M_2^2} \tag{3}$$

$$F_{a1} = -F_{xr} + F_{zr}sin(\rho) + F_{gr}sin(\rho) + F_s sin(\rho) \tag{4}$$

$$F_{r1} = F_{r2} + \sqrt{F_{yr}^2 + (F_{zr}cos(\rho))^2} \tag{5}$$

In this formulation, the weight of the rotor and hub (F_{zr}), the weight of the generator rotor (F_{gr}), and the weight of the main shaft (F_s) are obtained from RWT technical documents. Additionally, the relative distances between main bearings and component center of masses indicated on Figure 4 are provided in Section A. for each RWT. Torque (M_{xr}) and non-torque loads (M_{yr} and M_{zr}) are provided by the aero-elastic simulation at each time step.

C. Model Validation

The presented model is validated using pyFrame3DD, an open-source software for static and dynamic structural analysis obtained from the WISDEM repository.[34] It computes the static deflections, reactions, internal element forces, natural frequencies, mode shapes, and modal participation factors of two- and three-dimensional elastic structures using direct stiffness and mass assembly. The developed validation model uses pyFrame3DD to place two main bearing support points along the shaft and output reaction forces at these points. The upwind main bearing is restricted in the axial direction while the downwind main bearing remains floating, unable to react to axial loads. Moments are restricted in both main bearing in the y- and z-direction. For the hub forces and moments required for the validation program, low-speed-shaft loads, such as rotor torque, rotor thrust, and force/moments in the y- and z-directions were used from the aero-elastic simulation data, similar to the analytical model. In addition, the RWT parameters required for this program is shown in Table 9.

Table 9: pyFrame3DD Validation Parameters

Parameter	5-MW	10-MW	15-MW	Units
Length of Shaft	3	7.2	2.2	meters
Shaft thickness	0.25	0.45	0.2	meters
Shaft Diameter	0.75	3.13	5.8	meters
Tilt angle	5	5	6	degrees
Distance along shaft to MB1	0.2	1.801	0.9	meters
Distance along shaft to MB2	2.2	6.421	2.1	meters

D. L_{10} Formulation

The L_{10} life is the basis of calculating bearing life and reliability. Derived from the Lundberg-Palmgren hypothesis, the L_{10} value is the life, in millions of revolution, at which 90 percent of a bearing population will exceed without failing by rolling-element fatigue.[35]

$$L_{10} = \frac{C}{P_{eq}}^{e} \tag{6}$$

$$P_{eq} = XF_r + YF_a \tag{7}$$

$$L_{10} = \left[\frac{\Delta t}{T_{sim}} \sum_{t=0}^{N_t} \frac{1}{L_{10,t}}\right]^{-1} \tag{8}$$

The L_{10} life is calculated using Equation 6, where C is the dynamic load capacity, P_{eq} is the equivalent load, and e is the bearing exponent. The dynamic load capacity is a bearing specific parameter while e = 10/3 for roller bearings. As for the equivalent load, this value can be calculated using Equation 7, where X is the radial load factor and Y is the axial load factor. In order to account for the varying loads and speeds during wind turbine operation, the Palmgren-Langer-Miner rule is employed to obtain a single L_{10} value over time. This rule can be summarized through Equation 8, where T_n is the percentage of time elapsed in decimals and $L_{10,t}$ is the life calculation at each period of constant load and speed.

III. Results and Discussion

Using the methods describes in Section II., a bearing load time series is generated and compared to evaluate the accuracy of this model. The following graphs and analyses are generated using the modified 5-MW RWT parameters. The radial and axial forces on MB1 and the radial force on MB2 are calculated at each time step. The radial and axial forces for MB1 are combined using Equation 7 to obtain the total force. Finally, the L_{10} life is calculated for both bearings with the fatigue load time series and Equations 6 and 8.

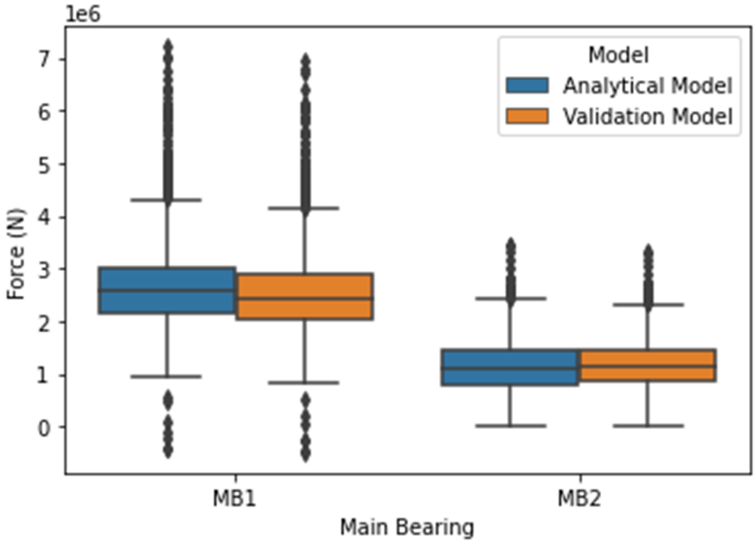

Figure 5: Comparative distribution of results between analytical and validation model

The order of magnitude of the loads generated through the developed model is consistent with previous studies.[24,29] Figure 5 compares the distribution of resulting loads from these two models, which shows good model agreement, evidenced by the similarity of means and distributions of the data. The error between the two models, measured by normalized root-mean-square error (RMSE), is 2.3% in MB1 total force and 2.9% in MB2 radial force. The discrepancy in MB1 total force is primarily contributed by discrepancies in the MB1 radial force, as shown in Figure 7. On the other hand, Figure 7 shows complete agreement in the axial direction because forces in axial direction are computed by simply adding the rotor thrust and the x-component of weights for both models, as previously shown in the model formulation.

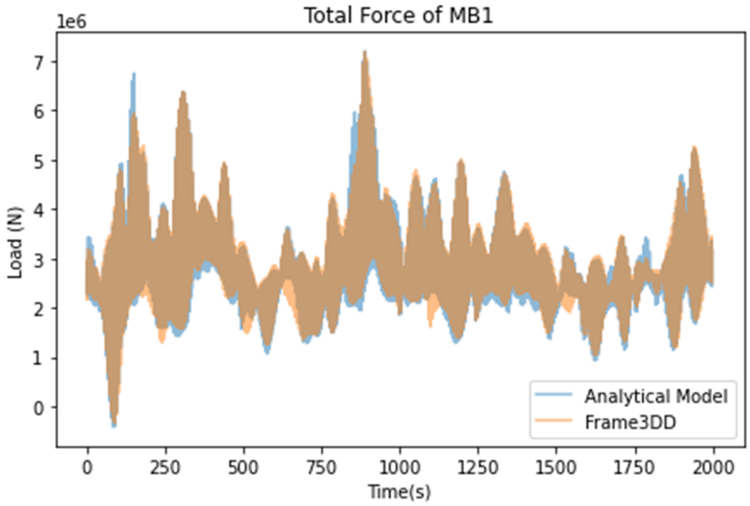

Figure 6: Example time series of total reaction force in MB1 from the analytical and validation models

The calculated errors seen in the radial force in MB1 (Figure 7) and radial force in MB2 (Figure 8) can be attributed to drivetrain parameters, number of nodes used in the validation model, and fundamental model differences. First, select parameters such as total shaft length, the distance from the hub flange to MB1, and material properties of the main shaft are required for the validation model. These parameters are not well defined in previous studies and therefore needed to be assumed for this study. Confirming these parameters and their consistency with the rest of the turbine design will improve the accuracy of the results. Second, the validation program breaks the main shaft into modal nodes. Increasing the number of nodes generally decreases these discrepancies seen in Figure 7 and Figure 8. For example, increasing the number of nodes from 15 to 90, we see the error in MB1 reduces to 1.9% and error in MB2 reduce to 2.3%, although this extends the run time of the validation model by 10 times for the given data set. The decrease in error is caused by the greater number of points of assessment along the main shaft which occurs when the number of nodes are increased. The bearings are modeled as a single-point support in the developed analytical model so adding more nodes makes the validation model increasingly consistent with the analytical model. Lastly, there are some fundamental differences in how these models generate their results. As opposed to the analytical model developed in this study, the validation model that uses pyFrame3DD does not consider or require the mass of the main shaft, rotor-hub, or generator. The analytical model processes hub loads, similar to the validation model, as well as the additional loads induced by the component masses. The analytical model does not consider the main shaft diameter, thickness, and material properties while the validation model does. Despite these model differences that affect how main bearing loads are computed, the models generate relatively consistent results.

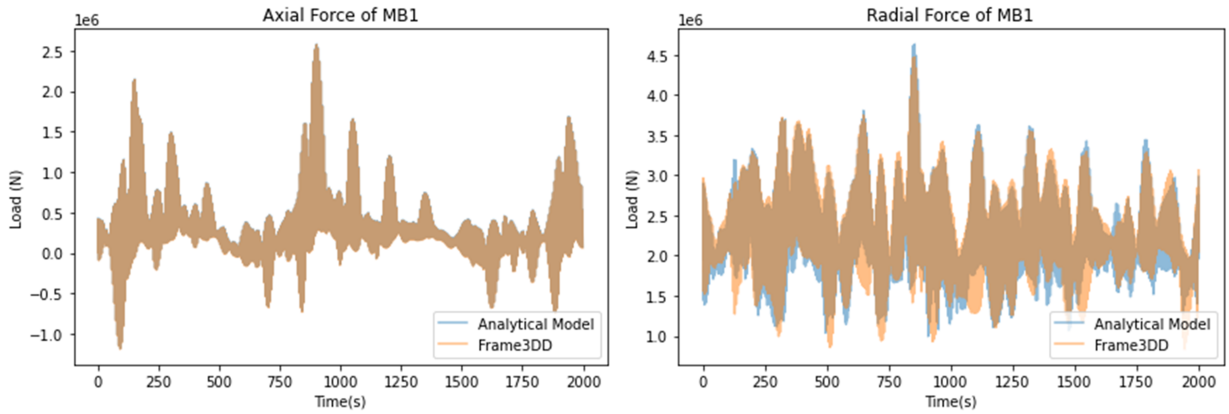

Figure 7: Example time series of reaction force in the radial and axial direction of MB1 from the analytical and validation models

The primary value of interest in this study is the L_{10} value. The L_{10} life of MB1 and MB2 is calculated to be 3.93 and 4.92 years, respectively. The error in forces does not significantly affect L_{10} values, as the difference in L_{10} life between the two models is approximately 2.6% or 200 hours. It is important to note that the L_{10} value is highly sensitive to the specifications of the bearing selected, and bearings for the 5-MW RWT were designed using methods defined in previous studies. Given that wind turbine main bearings last about 6 years,[9] the difference in life caused by model error is less than 1% of average bearing life and therefore considered negligible. Additionally, the run time for the validation model to compute bearing loads with this data set is approximately 30 seconds, while the analytical model requires less than 1 second, a 3000% improvement in computing time.

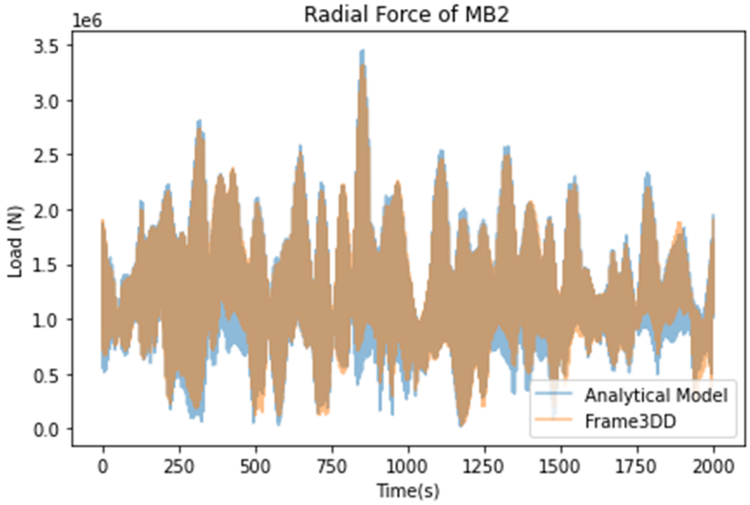

Figure 8: Example time series of reaction force in the radial direction of MB2 from the analytical and validation models

Despite its proven accuracy, the presented analytical model has some key limitations. The main bearings in this model do not react to moments because they are modelled as single-point, fixed supports. More detailed bearing dynamics for varying bearing designs could be considered in future work. Additionally, this model is specific to direct-drive,

double main bearing wind turbines. However, future work could consider varying main bearing configurations and gearbox wind turbines. Lastly, the results presented in this study are generated using one wind condition setting for a specific RWT. Future studies could consider varying wind conditions and the other RWTs presented in this study. Nonetheless, this study presents an effective method to estimate main bearing loads and reliability for double main bearing configurations of direct-drive wind turbines. The model generates results within approximately 2% of the validation model while significantly reducing the run time for the model.

IV. Conclusion

The main bearing remains a component prone to high failure rates and O&M costs. It is currently unclear how the degradation and reliability of main bearings are affected by offshore wind industry trends, especially as turbine designs move increasingly towards direct-drive systems. Additionally, component load and reliability analysis in simulations and at wind farm scale calls for a computationally inexpensive models. In this work, a main bearing analytical model is developed to estimate main bearing loads and reliability in direct-drive, offshore RWTs with double main bearings. This model employs open-source, RWT models of a 5-, 10-, and 15-MW design as well as aero-elastic simulation data to provide users an efficient, validated analytical model that is openly accessible for use. This model generates bearing loads and L_{10} life within approximately 2% of its higher-fidelity counterpart while reducing the run time by 3000%.

The tool developed in this study will enable researchers to integrate main bearing reliability in analyses that require many evaluations. The source code of this model is publicly available[36] to enable the uptake of others to use it in systems design and optimization studies, as well as O&M strategy simulations for bearing load estimation and life assessment. Reliability assessment throughout the design process is critical in reducing wind turbine failure and the associated costs, ensuring the advancement of offshore wind energy in the current energy market.

References

[1] Global Wind Energy Council. Global Wind Energy Report 2019. Technical report, 2020.

[2] Walter Musial, Philipp Beiter, Paul Spitsen, Jake Nunemaker, Vahan Gevorgian, Aubryn Cooperman, Rob Hammond, and Matt Shields. 2019 Offshore Wind Technology Data Update. Technical report, National Renewable Energy Laboratory (NREL), 10 2020.

[3] Faaij A. Junginger, M. and W. C Turkenburg. Cost Reduction Prospects for Offshore Wind Farms. Tech. Rep. 1, 2004.

[4] I. Dinwoodie, F. Quail, and D. McMillan. Analysis of offshore wind turbine operation & maintenance using a novel time domain meteo-ocean modeling approach. Proceedings of the ASME Turbo Expo, 6:847–857, 2012.

[5] Y. Sinha and J.A. Steel. A progressive study into offshore wind farm maintenance optimisation using risk based failure analysis. Renewable and Sustainable Energy Reviews, 42:735–742, 2 2015.

[6] James Carroll, Alasdair McDonald, and David McMillan. Failure rate, repair time and unscheduled O&M cost analysis of offshore wind turbines. Wind Energy, 19(6):1107–1119, 6 2016.

[7] Edward Hart, Benjamin Clarke, Gary Nicholas, Abbas Kazemi Amiri, James Stirling, James Carroll, Rob Dwyer-Joyce, Alasdair McDonald, and Hui Long. A review of wind turbine main bearings: Design, operation, modelling, damage mechanisms and fault detection. Wind Energy Science, 5(1):105–124, 2020.

[8] Edward Hart, Alan Turnbull, Julian Feuchtwang, David McMillan, Evgenia Golysheva, and Robin Elliott. Wind turbine main-bearing loading and wind field characteristics. Wind Energy, 22(11):1534–1547, 11 2019.

[9] D. Brake. WTG SRB Main Bearing Failures . Presented at the 2013 UVIG Wind Turbine/Plant Operations & Maintenance Users Group Meeting, 2013.

[10] Latha Sethuraman, Yi Guo, and Shuangwen Sheng. Main Bearing Dynamics in Three-Point Suspension Drivetrains for Wind Turbines. American wind energy association windpower, pages 18–21, 2015.

[11] Michael Horneman, Ashley Crowther, and Paul Dvorak. Establishing failure modes for bearings in wind turbines. Wind Engineering & Development, 2013.

[12] Matti Niclas Scheu, Lorena Tremps, Ursula Smolka, Athanasios Kolios, and Feargal Brennan. A systematic Failure Mode Effects and Criticality Analysis for offshore wind turbine systems towards integrated condition based maintenance strategies. Ocean Engineering, 176:118–133, 3 2019.

[13] F. Spinato, P.J. Tavner, G.J.W. van Bussel, and E. Koutoulakos. Reliability of wind turbine subassemblies. IET Renewable Power Generation, 3(4):387, 2009.

[14] Michael Wilkinson. Measuring Wind Turbine Reliability-Results of the Reliawind Project. Technical report, 2011.

[15] Berthold Hahn, Michael Durstewitz, and Kurt Rohrig. Reliability of wind turbines: Experiences of 15 years with 1,500 WTs WInD-Pool-Windenergie Informations-Datenpool View project IEA Wind TCP Task33-Reliability Data-Standardization of Data Collection for Wind Turbine Reliability and Maintenance Analyses View project Reliability of Wind Turbines Experiences of 15 years with 1,500 WTs. Technical report, 2006.

[16] Zhanwei Li, Binrong Wen, Zhike Peng, Xingjian Dong, and Yegao Qu. Dynamic modeling and analysis of wind turbine drivetrain considering the effects of non-torque loads. Applied Mathematical Modelling, 83:146–168, 7 2020.

[17] Wei Shi, Chang Wan Kim, Chin Wha Chung, and Hyun Chul Park. Dynamic modeling and analysis of a wind turbine drivetrain using the torsional dynamic model. International Journal of Precision Engineering and Manufacturing, 14(1):153–159, 2013.

[18] Jan Helsen, Pepijn Peeters, Klaas Vanslambrouck, Frederik Vanhollebeke, and Wim Desmet. The dynamic behavior induced by different wind turbine gearbox suspension methods assessed by means of the flexible multibody technique. Renewable Energy, 69:336–346, 9 2014.

[19] Caitlyn E Clark, Garrett E Barter, Kelsey Shaler, and Bryony Dupont. Reliability-Based Layout Optimization in Offshore Wind Energy Systems. In Preparation, 2020.

[20] Evan Gaertner, Jennifer Rinker, Latha Sethuraman, Frederik Zahle, Benjamin Anderson, Garrett E. Barter, Nikhar J. Abbas, Fanzhong Meng, Pietro Bortolotti, Witold Skrzypinski, George N. Scott, Roland Feil, Henrik Bredmose, Katherine Dykes, Matthew Shields, Christopher Allen, and Anthony Viselli. IEA Wind TCP Task 37: Definition of the IEA 15-Megawatt Offshore Reference Wind Turbine. 2020.

[21] The Timken Company. Part number ee755285 - 755367cd, tapered roller bearings - tdo (tapered double outer) imperial.

[22] Pietro Bortolotti, Helena Canet Tarres, Katherine Dykes, Karl Merz, Latha Sethuraman, David Verelst, and Frederik Zahle. IEA Wind TCP Task 37 Systems Engineering in Wind Energy-WP2.1 Reference Wind Turbines Technical Report. Technical report, 2019.

[23] Zahle F. Bitsche R. Kim T. Yde A. Henriksen L. C. Hansen M. H. Blasques J. P. A. A. Gaunaa M. Natarajan A.. Bak, C. The dtu 10-mw reference wind turbine, 2013.

[24] Ebbe Berge Smith. DESIGN AV NACELLE FOR EN 10 MW VINDTURBIN. NTNU Master Thesis, 2012.

[25] SKF Group. Bt2b 332497/ha4.

[26] SKF Group. 248/1800 cak30fa/w20.

[27] Latha Sethuraman, Yihan Xing, Zhen Gao, Vengatesan Venugopal, Markus Mueller, and Torgeir Moan. A 5MW direct-drive generator for floating spar-buoy wind turbine: Development and analysis of a fully coupled Mechanical model. Proceedings of the Institution of Mechanical Engineers, Part A: Journal of Power and Energy, 228(7):718–741, 11 2014.

[28] Jm Jonkman, S Butterfield, W Musial, and G Scott. Definition of a 5-MW reference wind turbine for offshore system development. Contract, (February):1–75, 2009.

[29] Amir Rasekhi Nejad, Yi Guo, Zhen Gao, and Torgeir Moan. Development of a 5 MW reference gearbox for offshore wind turbines. Wind Energy, (19):1089–1106, 2016.

[30] SKF Group. Bt2b 332493/ha4.

[31] SKF Group. 230/750 ca/w33.

[32] DNV/Riso. Guidelines for Design of Wind Turbines, volume 29. 2002.

[33] Jason Jonkman. Github Repo: OpenFast, 2020.

[34] Andrew Ning, Katherine Dykes, Pierre-Elouan Réthoré, and Garett Bart. The Wind-Plant Integrated System Design and Engineering Model (WISDEM), 2020.

[35] Erwin V Zaretsky. Rolling bearing life prediction, theory, and application. NASA Technical Reports, (November 2016):66, 2013.

[36] Daniyal Jamal. Github Repo: Main Bearing Analytical Model, 2020.